CHAPTER 7

TRANSMISSION LINES

Two-conductor transmission line theory is reviewed in this chapter. The conditions for transverse electromagnetic (TEM) wave propagation are examined. Topics covered include the distributed parameters of transmission lines, propagation constants, characteristic impedance, and reflection and transmission coefficients. Solutions for the frequency-domain current and voltage distributions on lossy and lossless lines, including the load response, are provided. The excitation of transmission lines by external electromagnetic fields is reviewed. Radiation from common-mode and differential-mode currents on transmission lines is examined.

7.1 EXAMPLES OF TRANSMISSION LINES

Transmission lines guide electromagnetic waves from a source to a load. The cross sections of some common types of transmission lines are illustrated in Fig. 7.1. Applications span the electromagnetic spectrum from ELF to SHF and include electric power distribution, cable TV systems, antenna systems, printed circuit boards, and microwave circuits.

All the examples in Fig. 7.1 are categorized as two-conductor transmission lines except for the multiconductor line. Two-conductor lines are analyzed by the methods of classical transmission line theory, which is reviewed in the following sections.

The analysis of multiconductor transmission lines is more formidable than the analysis of two-conductor lines and requires matrix methods and notation. The reader interested in multiconductor transmission lines is referred to the definitive work on the subject by Clayton Paul. See [1].

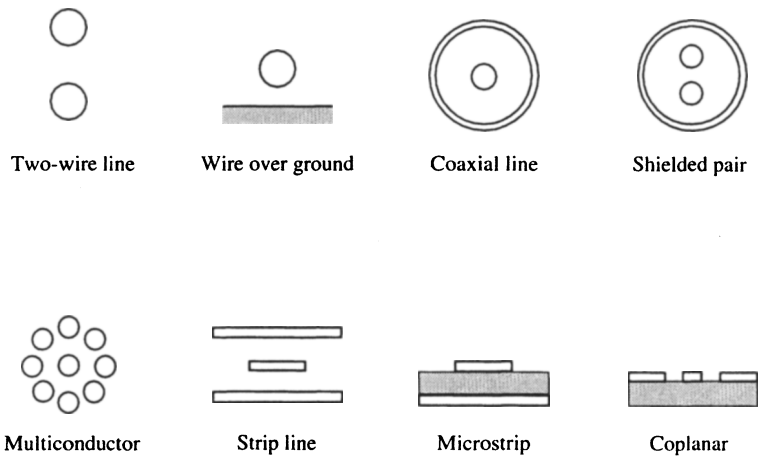

Figure 7.1 Cross sections of some common types of transmission lines.

7.2 TRANSVERSE ELECTROMAGNETIC (TEM) MODE OF PROPAGATION

Transmission line analysis is based on the basic assumption that the field surrounding the conductors is a transverse electromagnetic wave (TEM wave). A TEM wave is one in which both the electric and magnetic field vectors are perpendicular to the direction of propagation. That is, the longitudinal components of E and H are zero.

The TEM-wave assumption requires that the transmission line structure satisfy certain conditions in order for transmission line theory to be strictly applicable. Specifically,

- the line must be uniform
- the spacing between conductors must be electrically small
- the surrounding medium must be homogeneous
- the conductors must be lossless
- the currents on the line must be differential-mode currents.

These conditions are discussed below.

A *uniform line* is one in which the conductors are parallel to each other and have a uniform cross section along the line axis. Nonuniform lines have cross-sectional dimensions that vary along the line axis. Examples include tapered lines and lines with step discontinuities and gaps in the conductors.

The *spacing* between the conductors must be small compared to a wavelength. If the electrical spacing between conductors is large, generally in the order of one-half wavelength depending on the particular line geometry, higher order TE (transverse electric) and TM (transverse magnetic) modes of propagation will exist along with the TEM mode. If these *waveguide modes* exist, transmission line analysis alone will not predict the entire response. Another reason for the small- spacing requirement is to minimize radiation from differential-mode currents on unshielded lines.

Another condition for TEM-mode propagation is that the conductors must be surrounded by a *homogeneous medium.* An inhomogeneous surrounding medium might consist of several dielectrics or have a permittivity ε_r that varies with the radial or longitudinal position. This violates the TEM assumption since there is more than one velocity of propagation in the surrounding medium. If an effective dielectric constant can be calculated from the geometry and properties of the regions making up the medium, propagation on the line can be treated as propagation on an equivalent TEM line. This is referred to as a *quasi-TEM* solution. See [1] and [2].

The transmission line conductors must be *lossless* ($\sigma = \infty$). Lossy conductors invalidate the TEM assumption since currents flowing through a lossy conductor generate an electric field in the direction of propagation. If the losses are small, the TEM solution is approximately correct and is referred to as the *quasi-TEM* solution. The losses are accounted for by a distributed series resistance parameter, R.

Generally, both *differential-mode currents* and *common-mode currents* are present on a transmission line. This is illustrated in Fig. 7.2 for a two-conductor line. Transmission line theory and the TEM propagation mode assumption apply only to the differential-mode currents on the line. The differential-mode currents I_{DM} on the two conductors in Fig. 7.2 are, by definition, equal in magnitude and opposite in direction at any cross section in the line. The term differential mode is also referred to as transmission line mode, normal mode, metallic mode, bidirectional mode, and odd mode.

Common-mode currents I_{CM} on a transmission line driven by a voltage source can arise from asymmetries in the location of the source and load,

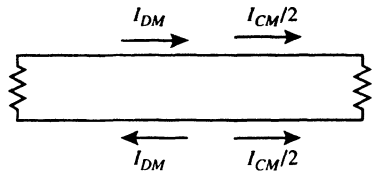

Figure 7.2 Differential-mode and common-mode currents on a two-conductor transmission line.

and from unbalances caused by the presence of nearby metal objects. See Paul [1]. Leakage through the shield of shielded cables can also produce common mode currents on the outer surface of the shield. These processes are referred to as differential-mode to common-mode conversion. The common mode current on a transmission line is distributed among the conductors. (In the case of multiconductor cables, the current is not necessarily distributed equally among the conductors since some of the interior conductors may be shielded by the outer conductors.) For the two-conductor line in Fig. 7.2, the common-mode currents on the conductors are equal in magnitude and flow in the same direction. The term common mode is also referred to as antenna mode, dipole mode, longitudinal mode, codirectional mode, and even mode.

Referring to Fig. 7.2, the response of a current probe clamped around both conductors would be

$$I_{DM} - I_{DM} + I_{CM}/2 + I_{CM}/2 = I_{CM}. \tag{7.1}$$

Only the differential-mode current flows in the terminating impedances. The common-mode current distribution is zero at both ends of the line.

Both common-mode currents and differential-mode currents can be *induced* on transmission lines by external electromagnetic fields. This subject is reviewed in Section 7.8.

Conversely, both common-mode and differential-mode currents on transmission lines are *sources* of radiated electromagnetic fields. The radiated fields produced by common-mode currents are much higher than the fields produced by like-magnitude differential-mode currents. Since differential-mode currents on the conductors flow in opposite directions, they tend to cancel; differential-mode radiation is proportional to the space-phase difference between the conductors. This topic is discussed in Section 7.9.

7.3 TWO-CONDUCTOR TRANSMISSION LINE MODEL

A two-conductor transmission line driven at one end and terminated at the other end is depicted schematically in Fig. 7.3. The conductors of the line are oriented parallel to the z-axis. The length of the line is s. The driving source at the sending end of the line has an open-circuit voltage V_G and an internal impedance Z_G. The line is terminated at the receiving end with a load impedance Z_L. $V(z)$ and $I(z)$ are the voltage and current distributions

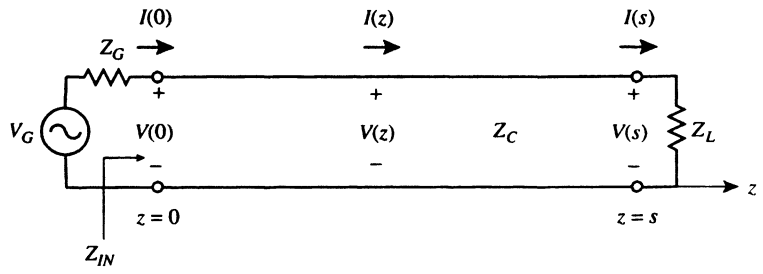

Figure 7.3 Schematic of a two-conductor transmission line with generator and load.

on the line. $V(0)$ and $I(0)$ are the voltage and current at the sending end of the line. $V(s)$ and $I(s)$ are the voltage and current at the receiving end, that is, the load voltage and load current. Z_C is the characteristic impedance of the line, and Z_{IN} is the input impedance.

The distributed parameters R, L, G, and C of a transmission line (see Section 7.4) determine the electrical properties of the line, the most important of which are (see Section 7.5):

- the *characteristic impedance* Z_C
- the *propagation constant* γ, consisting of
  - the *attenuation constant* α
  - and the *phase constant* β
- the *phase velocity* v.

The above electrical properties and the terminations at the ends of the line determine the following quantities (see Sections 7.6 and 7.7):

- the reflection and transmission coefficients
- the input impedance Z_{IN}
- the voltage and current distributions along the line $V(z)$ and $I(z)$
- and the terminal voltages and currents, $V(0)$, $I(0)$, $V(s)$, and $I(s)$.

7.4 DISTRIBUTED PARAMETERS

The equivalent circuit of a differential section dz of a two-conductor transmission line is shown in Fig. 7.4. The distributed circuit parameters, or

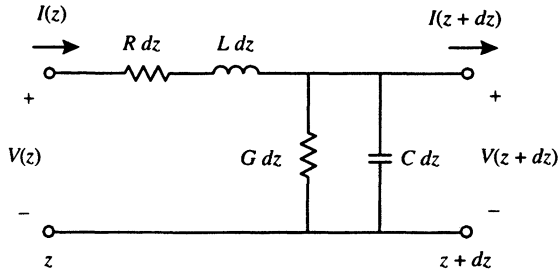

Figure 7.4 Equivalent circuit of a differential section of a two-conductor line.

per-unit-length parameters, are

R series resistance, ohms/meter
L series inductance, henrys/meter
G shunt conductance, mhos/meter
C shunt capacitance, farads/meter.

The series impedance per-unit-length is

$$Z = R + j\omega L \tag{7.2}$$

and the shunt admittance per-unit-length is

$$Y = G + j\omega C. \tag{7.3}$$

The basic differential equations for a uniform transmission line are derived from the equivalent circuit in Fig. 7.4. They are

$$\frac{d^2V}{dz^2} - ZYV = 0 \tag{7.4}$$

and

$$\frac{d^2I}{dz^2} - ZYI = 0. \tag{7.5}$$

Equations (7.4) and (7.5) are sometimes referred to as the *Telegrapher's equations.*

7.5 PROPAGATION CONSTANT AND CHARACTERISTIC IMPEDANCE

The solutions for the voltage and current in (7.4) and (7.5) take the following forms:

$$V = V_1\varepsilon^{j\omega t}\varepsilon^{\gamma z} + V_2\varepsilon^{j\omega t}\varepsilon^{-\gamma z} \tag{7.6}$$

and

$$I = \frac{V_1}{Z_C}\varepsilon^{j\omega t}\varepsilon^{\gamma z} - \frac{V_2}{Z_C}\varepsilon^{j\omega t}\varepsilon^{-\gamma z}. \tag{7.7}$$

The quantity γ is called the *propagation constant*, defined by

$$\boxed{\gamma = \alpha + j\beta = \sqrt{ZY} = \sqrt{(R + j\omega L)(G + j\omega C)}} \tag{7.8}$$

where α is the *attenuation constant*, nepers/m
β is the *phase constant*, rad/m.

The *attenuation constant in dB per meter*, denoted by $\alpha_{\text{dB/m}}$, is

$$\boxed{\alpha_{\text{dB/m}} = 8.686\alpha.} \tag{7.9}$$

(One neper is equivalent to 8.686 dB. The difference arises from the definition of the two units. The neper is equal to the natural logarithm of the ratio of two voltages or currents, while the decibel is equal to 20 times the logarithm to the base ten of the ratio of two voltages or currents.)

The quantity Z_C in (7.7) is the *characteristic impedance* of the line and is defined by

$$\boxed{Z_C = \sqrt{\frac{Z}{Y}} = \sqrt{\frac{R + j\omega L}{G + j\omega C}} \quad \text{ohms.}} \tag{7.10}$$

If $\alpha + j\beta$ is substituted for γ in (7.6) and (7.7), these equations assume the following form:

$$V = V_1\varepsilon^{\alpha z}\varepsilon^{j(\omega t+\beta z)} + V_2\varepsilon^{-\alpha z}\varepsilon^{j(\omega t-\beta z)} \tag{7.11}$$

and

$$I = \frac{V_1}{Z_C}\varepsilon^{\alpha z}\varepsilon^{j(\omega t+\beta z)} - \frac{V_2}{Z_C}\varepsilon^{-\alpha z}\varepsilon^{j(\omega t-\beta z)}. \tag{7.12}$$

The first terms in (7.11) and (7.12) are *backward-traveling waves* on the transmission line, traveling in the $-z$ direction. The second terms in (7.11) and (7.12) are *forward-traveling waves* on the line, traveling in the $+z$ direction. The terms V_1 and V_2 are complex-valued constants that are determined by the terminal conditions at the ends of the line.

The terms $\varepsilon^{\alpha z}$ and $\varepsilon^{-\alpha z}$ represent the attenuation of the backward-traveling and forward-traveling wave amplitudes, respectively. For example, the attenuation over a segment of line of length l is, by definition, the ratio of the amplitudes of the traveling wave at the beginning and the end

of the segment, or

$$\frac{V(z)}{V(z+l)} = \frac{\varepsilon^{-\alpha z}}{\varepsilon^{-\alpha(z+l)}} = \varepsilon^{\alpha l} \tag{7.13}$$

where α = the attenuation constant, nepers per meter.

The attenuation in nepers is

$$\ln \varepsilon^{\alpha l} = \alpha l \qquad \text{nepers.} \tag{7.14}$$

The attenuation in dB is

$$20 \log \varepsilon^{\alpha l} = 8.686 \alpha l = \alpha_{\text{dB/m}} l \qquad \text{dB.} \tag{7.15}$$

The velocity of propagation of the waves on a transmission line, referred to as the phase velocity, is obtained from (7.11) and (7.12) by equating the phase angle $(\omega t - \beta z)$ to a constant and taking the time derivative. See Johnson [3]. The result is

$$\omega - \beta \frac{dz}{dt} = 0. \tag{7.16}$$

The phase velocity is $v = dz/dt$, or

$$\boxed{v = \frac{\omega}{\beta} \qquad \text{m/sec}} \tag{7.17}$$

where $\omega = 2\pi f$, radian frequency
$\beta = 2\pi/\lambda$, phase constant
$\lambda = v/f$, wavelength on the line.

Lossless Lines

A lossless transmission line is one with perfect conductors ($\sigma = \infty$) and a lossless surrounding medium (the permittivity ε is real). On a lossless line, the characteristic impedance is real and the attenuation constant is zero. Most physically short radio frequency lines can be considered lossless. On a lossless line, $R = 0$ and $G = 0$ and the series impedance per-unit-length and shunt admittance per-unit-length in (7.2) and (7.3) reduce to

$$Z = j\omega L \tag{7.18}$$

and

$$Y = j\omega C. \tag{7.19}$$

The propagation constant, (7.8), for a lossless line becomes

$$\boxed{\gamma = j\beta = j\omega\sqrt{LC}.} \tag{7.20}$$

The attenuation constant $\alpha = 0$, and the phase constant is

$$\boxed{\beta = \omega\sqrt{LC} = \omega\sqrt{\mu\varepsilon} = 2\pi/\lambda \qquad \text{rad/sec}} \tag{7.21}$$

where μ permeability of the medium
ε permittivity of the medium
λ wavelength on the line.

The characteristic impedance, (7.10), for a lossless line is

$$\boxed{Z_C = \sqrt{\frac{L}{C}} \qquad \text{ohms.}} \tag{7.22}$$

The *wave impedance* Z_w of the TEM wave on a transmission line (see Section 2.12 in Chapter 2) is equal to the intrinsic impedance of the medium and is given by

$$\boxed{Z_W = \sqrt{\frac{\mu}{\varepsilon}}.} \tag{7.23}$$

If the surrounding medium is air, the wave impedance is that of free space:

$$\boxed{Z_o = \sqrt{\frac{\mu_o}{\varepsilon_o}}.} \tag{7.24}$$

The characteristic impedance of a transmission line, defined as the ratio of the voltage between the conductors to the current flowing on the conductors, is a function of the geometry of the line *and* the medium. The wave impedance, defined as the ratio of the transverse electric and magnetic fields, is a function of the surrounding medium only. Collin [4] has shown that the characteristic and wave impedances are related by

$$Z_C = \frac{\varepsilon}{C} Z_W. \tag{7.25}$$

The phase velocity for a lossless line, from (7.17) and (7.21), is

$$\boxed{v = \frac{\omega}{\beta} = \frac{1}{\sqrt{LC}} = \frac{1}{\sqrt{\mu\varepsilon}} \qquad \text{m/sec}} \tag{7.26}$$

where μ and ε are the permeability and permittivity of the surrounding dielectric medium. (For a lossless line, the product LC depends *only*

on the permeability and permittivity of the surrounding medium, and is independent of the size and spacing of the conductors.)

Lossy Lines at Radio Frequencies

At radio frequencies, $\omega L \gg R$ and $\omega C \gg G$. Depending on the particular line, these inequalities are adequately satisfied at frequencies above a few kilohertz to a few hundred kilohertz. Using these inequalities, the characteristic impedance (7.10) and phase velocity (7.17) on radio frequency lines reduce to the same form as lossless lines:

$$\boxed{Z_C = \sqrt{\frac{L}{C}} \quad \text{ohms.}} \tag{7.27}$$

$$\boxed{v = \frac{1}{\sqrt{LC}} \quad \text{m/sec.}} \tag{7.28}$$

At radio frequencies, Z_C and v are transmission line "constants" since L and C are independent of frequency.

The propagation constant on radio frequency lines is well approximated by

$$\boxed{\gamma = \left[\frac{R}{2Z_C} + \frac{GZ_C}{2}\right] + j\omega\sqrt{LC}} \tag{7.29}$$

where the attenuation constant is

$$\boxed{\alpha(\omega) = \frac{R}{2Z_C} + \frac{GZ_C}{2} \quad \text{neper/m}} \tag{7.30}$$

and the phase constant is

$$\boxed{\beta = \omega\sqrt{LC} \quad \text{rads/m.}} \tag{7.31}$$

The attenuation constant $\alpha(\omega)$ increases with frequency since both distributed circuit parameters R and G increase with frequency. The series resistance R increases as the square root of frequency while G increases linearly with frequency. The first term in (7.30) is the losses in the conductors, while the second term is the dielectric losses. See Table 7.1.

Calculation of Transmission Line Constants

The electrical constants Z_C, α, β, v, and λ are functions of the per-unit-length parameters R, L, C, and G, which in turn are determined by the

Table 7.1 Design Equations for Two-Wire and Coaxial Lines at Radio Frequencies

Quantity	Two-wire line Fig. 7.5(a)	Coaxial line Fig. 7.5(b)	Units
R	$\frac{2}{a}\sqrt{\frac{f\mu}{\pi\sigma}}$	$\sqrt{\frac{f\mu}{4\pi\sigma}}\left(\frac{1}{a}+\frac{1}{b}\right)$	ohms/m
L	$\frac{\mu}{\pi}\ln\frac{2b}{a}$	$\frac{\mu}{2\pi}\ln\frac{b}{a}$	henrys/m
C	$\frac{\pi\varepsilon}{\ln(2b/a)}$	$\frac{2\pi\varepsilon}{\ln(b/a)}$	farads/m
G	$2\pi fC\tan\delta$	$2\pi fC\tan\delta$	mhos/m
Z_C	$\frac{120}{\sqrt{\varepsilon_r}}\ln\frac{2b}{a}$	$\frac{60}{\sqrt{\varepsilon_r}}\ln\frac{b}{a}$	ohms
α	$\frac{R}{2Z_C}+\frac{GZ_C}{2}$	$\frac{R}{2Z_C}+\frac{GZ_C}{2}$	nepers/m
v	$\frac{3\times10^8}{\sqrt{\varepsilon_r}}$	$\frac{3\times10^8}{\sqrt{\varepsilon_r}}$	m/sec

$\varepsilon=\varepsilon_0\varepsilon_r$ permittivity of dielectric medium, farads/m
$\mu=\mu_0\mu_r$ permeability of conductors, henrys/m
σ = conductivity of conductors, mhos
$\tan\delta$ = loss tangent of dielectric medium

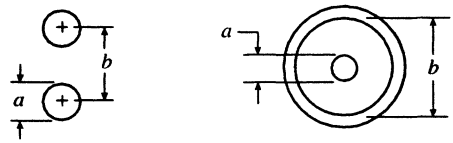

(a) Two-wire line (b) Coaxial line

Figure 7.5 Cross-sectional dimensions of a two-wire line and a coaxial line.

geometry of the line, the conductivity and permeability of the conductors, and the permittivity of the dielectric medium.

The design equations for two-wire and coaxial lines are summarized in Table 7.1. The derivations for simple transmission line geometries can be found, for example, in the texts by Johnson [3] and Chipman [6].

Design data for more complex configurations such as shielded pairs, multiconductor cables, coplanar, strip, and microstrip lines (and their many variations), may be found in the excellent design handbook by Wadell [2], in the book by Paul [1] on multiconductor cables, and in the chapter by Itoh in [5].

In any case, the numerical calculation of transmission line parameters and constants requires a knowledge of the properties of the materials, which is the purview of designers. The user of transmission lines can usually obtain the necessary data from the manufacturers. Specifically, manufacturers publish data on the characteristic impedance, the attenuation constant, and the phase velocity (as a percentage of the speed of light in a vacuum).

7.6 REFLECTION AND TRANSMISSION COEFFICIENTS

Refer to Figure 7.3. When a wave is launched by the generator, it travels toward the load with velocity v. The time it takes this incident wave to reach the load is $T = s/v$. If the load impedance is not matched to the characteristic impedance of the line ($Z_L \neq Z_C$), part of the incident wave is reflected and travels back toward the sending end of the line. If the generator impedance is not matched to the characteristic impedance ($Z_G \neq Z_C$), the reflected wave is re-reflected and travels forward toward the load, and so on, until a state of equilibrium is reached. For a single input pulse, the waves traveling back and forth on the line attenuate and eventually die out. When the input is a sine wave, a steady-state condition is eventually reached. Solutions for the steady-state voltages and currents for sinusoidal excitations are given in the following section.

The total voltage $V(z)$ at any point on the line is the sum of the incident voltage wave $V^+(z)$ traveling in the $+z$ direction and the reflected voltage wave $V^-(z)$ traveling in the $-z$ direction. This is illustrated in Fig. 7.6. Thus,

$$V(z) = V^+(z) + V^-(z). \tag{7.32}$$

The current at any point on the line is also the sum of two waves traveling in opposite directions:

$$I(z) = I^+(z) + I^-(z). \tag{7.33}$$

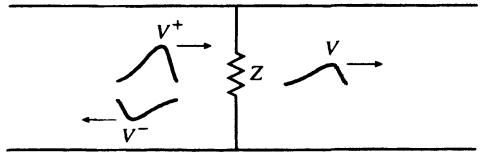

Figure 7.6 Incident, reflected, and transmitted voltages.

The incident and reflected voltages and currents are related by the characteristic impedance:

$$V^+(z) = Z_C I^+(z) \tag{7.34}$$

$$V^-(z) = -Z_C I^-(z). \tag{7.35}$$

The ratio of reflected and incident voltage waves at any point on the line is called the *voltage reflection coefficient*, denoted $\rho^V(z)$:

$$\rho^V(z) = \frac{V^+(z)}{V^-(z)}. \tag{7.36}$$

The receiving-end and sending-end *voltage reflection coefficients* are

$$\rho_L^V = \frac{V^-(s)}{V^+(s)} = \frac{Z_L - Z_C}{Z_C + Z_L} \qquad \text{receiving end} \tag{7.37}$$

$$\rho_G^V = \frac{V^-(0)}{V^+(0)} = \frac{Z_G - Z_C}{Z_C + Z_G} \qquad \text{sending end.} \tag{7.38}$$

The ratio of reflected and incident current waves at any point on the line is called the *current reflection coefficient*, denoted $\rho^I(z)$:

$$\rho^I(z) = \frac{I^+(z)}{I^-(z)}. \tag{7.39}$$

The current reflection coefficient is the negative of the voltage reflection coefficient: See (7.34) and (7.35).

The receiving-end and sending-end *current reflection coefficients* are

$$\rho_L^I = -\rho_L^V = \frac{Z_C - Z_L}{Z_C + Z_L} \qquad \text{receiving end} \tag{7.40}$$

$$\rho_G^I = -\rho_G^V = \frac{Z_C - Z_G}{Z_C + Z_G} \qquad \text{sending end.} \tag{7.41}$$

The ratio of the total voltage at an impedance (or discontinuity) to that of the incident voltage wave is called the *voltage transmission coefficient*, denoted τ^V. See Fig. 7.6. That is, at the impedance

$$\tau^V = \frac{V}{V^+} \tag{7.42}$$

or

$$V = \tau^V V^+. \tag{7.43}$$

The impedance may be a lumped element at either end of the line, or it may represent the impedance at the junction with another section of line. In the latter case, (7.43) is the voltage V transmitted beyond the junction.

The receiving-end and sending-end *voltage transmission coefficients* are

$$\tau_L^V = \frac{V(s)}{V^+(s)} = 1 + \rho_L^V = \frac{2Z_L}{Z_C + Z_L} \qquad \text{receiving end} \tag{7.44}$$

$$\tau_G^V = \frac{V(0)}{V^-(0)} = 1 + \rho_G^V = \frac{2Z_G}{Z_C + Z_G} \qquad \text{sending end.} \tag{7.45}$$

The *current transmission coefficients* are

$$\tau_L^I = 1 + \rho_L^I = \frac{2Z_C}{Z_C + Z_L} \qquad \text{receiving end} \tag{7.46}$$

$$\tau_G^I = 1 + \rho_G^I = \frac{2Z_C}{Z_C + Z_G} \qquad \text{sending end.} \tag{7.47}$$

The reflection and transmission coefficients for voltages and currents on transmission lines are analogous to the plane-wave reflection and transmission coefficients defined in Section 2.6 in Chapter 2.

7.7 SINUSOIDAL STEADY-STATE SOLUTIONS

In this section, we review the frequency-domain solutions for the voltages and currents on the two-wire transmission line illustrated in Fig. 7.3. The output of the generator V_G is a sine wave that has been applied for a sufficient time so that steady-state conditions obtain.

Voltage and Current Distributions

The voltage and current distributions on the line in Fig. 7.3, expressed in *exponential form*, are [1], [3]

$$V(z) = V_G \frac{Z_C}{Z_C + Z_G} \frac{1 + \rho_L^V \varepsilon^{-2\gamma s} \varepsilon^{2\gamma z}}{1 - \rho_L^V \rho_G^V \varepsilon^{-2\gamma s}} \varepsilon^{-\gamma z} \tag{7.48}$$

$$I(z) = V_G \frac{1}{Z_C + Z_G} \frac{1 + \rho_L^I \varepsilon^{-2\gamma s} \varepsilon^{2\gamma z}}{1 - \rho_L^I \rho_G^I \varepsilon^{-2\gamma s}} \varepsilon^{-\gamma z} \tag{7.49}$$

where $\rho^I = -\rho^V$.

The impedance at any point on the line is

$$Z(z) = \frac{V(z)}{I(z)} = Z_C \frac{1 + \rho_L^V \varepsilon^{-2\gamma s} \varepsilon^{2\gamma z}}{1 + \rho_L^I \varepsilon^{-2\gamma s} \varepsilon^{2\gamma z}}. \tag{7.50}$$

Note that $Z(z)$ is a function of the characteristic impedance and the load reflection coefficient, but is independent of the sending-end reflection coefficient and impedance Z_G.

The exponential forms of the solutions are explicit functions of the propagation constant γ and the reflection coefficients of the load and source, ρ_L and ρ_G.

The voltage and current distributions on the line in Fig. 7.3, expressed in *hyperbolic notation*, are

$$V(z) = V_G \frac{Z_C Z_L \cosh \gamma(s-z) + Z_C^2 \sinh \gamma(s-z)}{(Z_C Z_G + Z_C Z_L)\cosh \gamma s + (Z_C^2 + Z_G Z_L)\sinh \gamma s} \tag{7.51}$$

$$I(z) = V_G \frac{Z_C \cosh \gamma(s-z) + Z_L \sinh \gamma(s-z)}{(Z_C Z_G + Z_C Z_L)\cosh \gamma s + (Z_C^2 + Z_G Z_L)\sinh \gamma s} \tag{7.52}$$

and the impedance at any point on the line is

$$Z(z) = \frac{V(z)}{I(z)} = Z_C \frac{Z_L + Z_C \tanh \gamma(s-z)}{Z_C + Z_L \tanh \gamma(s-z)}. \tag{7.53}$$

Again, $Z(z)$ is a function of the characteristic impedance and load impedance, but independent of Z_G. It is sometimes referred to as the impedance looking toward the load, or the input impedance at point z.

Voltages and Currents at the Terminations

The *load voltage* or *receiving-end voltage* is found from (7.51) by setting $z = s$. The result is

$$V(s) = \frac{V_G Z_C Z_L}{(Z_C Z_G + Z_C Z_L)\cosh \gamma s + (Z_C^2 + Z_G Z_L)\sinh \gamma s}. \tag{7.54}$$

The *sending-end voltage* (i.e., the voltage at the input to the line) is given by (7.51) with $z = 0$. We have

$$V(0) = V_G \frac{Z_C Z_L \cosh \gamma s + Z_C^2 \sinh \gamma s}{(Z_C Z_G + Z_C Z_L)\cosh \gamma s + (Z_C^2 + Z_G Z_L)\sinh \gamma s}. \tag{7.55}$$

The *voltage across the sending-end impedance* Z_G is

$$V_{Z_G} = V_G - V(0) \tag{7.56}$$

or

$$V_{Z_G} = V_G \frac{Z_C Z_G \cosh \gamma s + Z_G Z_L \sinh \gamma s}{(Z_C Z_G + Z_C Z_L)\cosh \gamma s + (Z_C^2 + Z_G Z_L)\sinh \gamma s}. \tag{7.57}$$

The *load current* or *receiving-end current* is found from (7.52) by setting $z = s$. The result is

$$I(s) = \frac{V_G Z_C}{(Z_C Z_G + Z_C Z_L)\cosh \gamma s + (Z_C^2 + Z_G Z_L)\sinh \gamma s}. \tag{7.58}$$

The *sending-end current* (i.e., the current flowing in the impedance Z_G) is found from (7.52) with $z = 0$. Thus,

$$I(0) = V_G \frac{Z_C \cosh \gamma s + Z_L \sinh \gamma s}{(Z_C Z_G + Z_C Z_L) \cosh \gamma s + (Z_C^2 + Z_G Z_L) \sinh \gamma s}. \tag{7.59}$$

The *input impedance* or *sending-end impedance* Z_{IN} of the transmission line is obtained from (7.53) with $z = 0$. See Fig. 7.3. The result is

$$Z_{IN} = Z_C \frac{Z_L + Z_C \tanh \gamma s}{Z_C + Z_L \tanh \gamma s}. \tag{7.60}$$

Matched Load. When the load impedance is matched to the characteristic impedance of the transmission line ($Z_L = Z_C$), the load reflection coefficients are zero ($\rho_L^V = \rho_L^I = 0$) and all of the incident power is absorbed by the load.

The receiving-end (load) voltage and current, the sending-end voltage and current, and the input impedance on a line with a matched load impedance are given in Table 7.2 for both lossy and lossless lines.

For the matched load case, the exponential form of the load voltage and load current is given since this form readily conveys the physical picture of the incident wave having propagated down the length of the line.

Table 7.2 Terminal Voltages and Currents and Input Impedance for a Matched Load

Matched load	
Lossy Line	**Lossless Line**
$V(s) = \frac{V_G Z_L}{Z_L + Z_G} \varepsilon^{-as} \varepsilon^{-j\beta s}$	$V(s) = \frac{V_G Z_L}{Z_L + Z_G} \varepsilon^{-j\beta s}$
$I(s) = \frac{V_G}{Z_L + Z_G} \varepsilon^{-as} \varepsilon^{-j\beta s}$	$I(s) = \frac{V_G}{Z_L + Z_G} \varepsilon^{-j\beta s}$
$V(0) = \frac{V_G Z_L}{Z_L + Z_G}$	
$I(0) = \frac{V_G}{Z_L + Z_G}$	
$Z_{IN} = Z_L = Z_C$	

The attenuation on the line in dB, from (7.15), is

$$20 \log \varepsilon^{\alpha s} = 8.686 \alpha s = \alpha_{\text{dB/m}} s \qquad \text{dB} \tag{7.61}$$

where s is the length of the line in meters. α is the attenuation constant in nepers/meter, and $\alpha_{\text{dB/m}}$ is the attenuation constant in dB/m. If the line is lossless, $\alpha = 0$ and $\gamma = j\beta$.

Open-Circuit Load. When the load impedance is an open-circuit ($Z_L = \infty$), the load reflection coefficients are $\rho_L^V = +1$ and $\rho_L^I = -1$, and all of the incident power is reflected by the load.

The receiving-end (load) voltage and current, the sending-end voltage and current, and the input impedance on a line with an open-circuit load impedance are given in Table 7.3 for both lossy and lossless lines.

Table 7.3 Terminal Voltages and Currents and Input Impedance for an Open-Circuit Load

Open-circuit load	
Lossy Line	**Lossless Line**
$V(s) = \dfrac{V_G Z_C}{Z_C \cosh \gamma s + Z_G \sinh \gamma s}$	$V(s) = \dfrac{V_G Z_C}{Z_C \cos \beta s + jZ_G \sin \beta s}$
$I(s) = 0$	
$V(0) = \dfrac{V_G Z_C}{Z_C + Z_G \tanh \gamma s}$	$V(0) = \dfrac{V_G Z_C}{Z_C + jZ_G \tan \beta s}$
$I(0) = \dfrac{V_G \tanh \gamma s}{Z_C + Z_G \tanh \gamma s}$	$I(0) = \dfrac{jV_G \tan \beta s}{Z_C + jZ_G \tan \beta s}$
$Z_{IN} = Z_C \coth \gamma s$	$Z_{IN} = -jZ_C \cot \beta s$

For the open-circuit case, the hyperbolic form of the solutions is given since this form is more compact when reflections exist on the line.

Short-Circuit Load. When the load impedance is a short-circuit ($Z_L = 0$), the load reflection coefficients are $\rho_L^V = -1$ and $\rho_L^I = +1$. As is the case with an open-circuit load, all of the incident power is reflected by the load.

The receiving-end (load) voltage and current, the sending-end voltage and current, and the input impedance on a line with a short-circuit load impedance are given in Table 7.4 for both lossy and lossless lines.

Table 7.4 Terminal Voltages and Currents and Input Impedance for a Short-Circuit Load

Short-circuit load	
Lossy Line	**Lossless Line**
$V(s) = 0$	
$I(s) = \dfrac{V_G}{Z_G \cosh \gamma s + Z_C \sinh \gamma s}$	$I(s) = \dfrac{V_G}{Z_G \cos \beta s + jZ_C \sin \beta s}$
$V(0) = \dfrac{V_G Z_C \sinh \gamma s}{Z_G \cosh \gamma s + Z_C \sinh \gamma s}$	$V(0) = \dfrac{jV_G Z_C \sin \beta s}{Z_G \cos \beta s + jZ_C \sin \beta s}$
$I(0) = \dfrac{V_G \cosh \gamma s}{Z_G \cosh \gamma s + Z_C \sinh \gamma s}$	$I(0) = \dfrac{V_G \cos \beta s}{Z_G \cos \beta s + jZ_C \sin \beta s}$
$Z_{IN} = Z_C \tanh \gamma s$	$Z_{IN} = jZ_C \tan \beta s$

Voltage Standing-Wave Ratio (VSWR)

When the load impedance and characteristic impedance are mismatched ($Z_L \neq Z_C$), part of the incident energy is reflected at the load. The interference between incident and reflected waves results in *standing waves* of voltage and current on the transmission line.

This is illustrated in Fig. 7.7. In this example, a 5-m length of 75-ohm coaxial cable (RG-11A/U) connects a 50-ohm generator to a 50-ohm load. The amplitude of the generator is 1 V, and the frequency is 150 MHz.

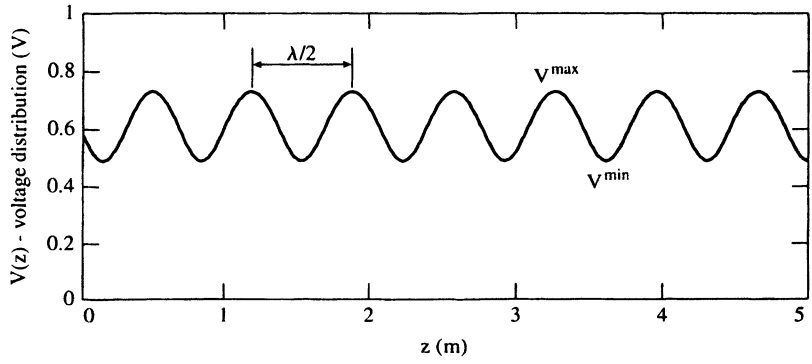

Figure 7.7 Voltage standing-wave pattern on the 5-m coaxial cable.

Referring to Fig. 7.3,

$V_G = 1$ volt	generator voltage
$s = 5$ m	length of cable
$Z_C = 75$ ohms	characteristic impedance
$Z_G = 50$ ohms	generator impedance (sending-end termination)
$Z_L = 50$ ohms	load impedance
$f = 150$ MHz	frequency.

The phase velocity of the coaxial cable is 69.5 percent of the speed of light in a vacuum. Thus

$$v = 0.695c = 0.695 \times 3 \times 10^8 \text{ m/s} = 209 \times 10^6 \text{ m/s}.$$

The wavelength on the line is

$$\lambda = \frac{v}{f} = \frac{209 \times 10^6}{150 \times 10^6} = 1.39 \text{ m}.$$

The phase constant is

$$\beta = \frac{2\pi}{\lambda} = \frac{2\pi}{1.39} = 2\pi \times 0.719 \qquad \text{rads/m}.$$

The attenuation constant for the RG-11A/U coaxial cable is 3 dB per 100 ft (0.0984 dB/m) at 150 MHz [5]. The total attenuation for the 5-m length of cable is 0.5 dB, which is negligible for purposes of this example. Thus, $\alpha \approx 0$.

Using these values, the voltage distribution $V(z)$ on the coaxial cable was calculated using (7.51) with $\alpha = 0$, $\gamma = j\beta$ (lossless case). The result is plotted in Fig. 7.7. The peaks of the voltage standing- wave are spaced one-half wavelength apart. (A similar plot of the current standing-wave would be 180° out of phase with the voltage standing-wave, i.e., the current maximums would correspond to voltage minimums.)

The *voltage standing-wave ratio* Γ is defined as the ratio of the maximum-to-minimum voltage of the standing-wave on the transmission line:

$$\Gamma = \frac{V^{\max}}{V^{\min}} \qquad \text{VSWR}. \tag{7.62}$$

The VSWR of the line in Fig. 7.7 is $\Gamma = 1.5$.

The VSWR is related to the voltage reflection coefficient of the load by [also see (4.28) to (4.30) in Section 4.1]

$$\boxed{\Gamma = \frac{1 + |\rho_L^V|}{1 - |\rho_L^V|}.} \tag{7.63}$$

Conversely, the receiving-end voltage reflection coefficient in terms of the VSWR is

$$\boxed{|\rho_L^V| = \frac{\Gamma - 1}{\Gamma + 1}.} \tag{7.64}$$

7.8 EXCITATION BY EXTERNAL ELECTROMAGNETIC FIELDS

Equations for the response of a two-wire transmission line illuminated by a nonuniform electromagnetic field were presented in the seminal paper by Taylor, Satterwhite, and Harrison [7]. A more compact form of the equations, easier to solve and allowing a clearer physical interpretation, was derived in [8]. Applications of the theory for two-conductor lines, including a conductor over a ground plane and shielded cables, can be found in the book by the author [9]. The coupling theory was extended to multiconductor lines by Paul [10]. The driving sources in all of these models are the normal component of the incident magnetic field H_y^i and the transverse component of the incident electric field E_x^i (see Fig. 7.9). The solutions are expressed in terms of the line current $I(z)$ and *total voltage* $V(z)$ on the line. This is the formulation that will be used in this section.

There are two alternative, but equivalent, forms of the solutions. In the form developed by Agrawal, Price, and Gurbaxani [11], the driving sources are the incident electric field components tangential to the conductors and to the terminations. The solutions are expressed in terms of the line current $I(z)$ and *scattered voltage* $V^s(z)$ on the line. In the formulation developed by Rachidi [12], the driving sources are the incident magnetic field components.

Those readers wishing to pursue the theory in more depth are referred to the previously mentioned book by Paul [1] and to the book by Tesche, Ianoz, and Karlsson [13]. In the book by Paul [1], general solutions for the response of two-conductor and multiconductor transmission lines to

incident electromagnetic fields in both the time and frequency domains are developed. In the book by Tesche, et al., [13], a thorough theoretical analysis of field coupling to two-conductor lines, a conductor over a ground plane, and shielded cables is presented.

In the remainder of this section, the frequency-domain solutions for the load currents of a lossless two-conductor line and a conductor over a ground plane are reviewed.

Two-Conductor Line

A nonuniform electromagnetic field incident on a uniform two-conductor transmission line is depicted in Fig. 7.8. $E^i(x, y, z)$ and $H^i(x, y, z)$ are the electric and magnetic field components of the incident field. The transmission line lies in the x-z plane. The length of the line is s, the spacing between the conductors is b, and the diameter of the conductors is a [see Fig. 7.5(a)]. The characteristic impedance is Z_C. (See Table 7.1 for calculation of Z_C in terms of the line geometry and dielectric constant of the surrounding dielectric medium.) In keeping with the notation in the previous sections, Z_G and Z_L are the left-hand and right-hand load impedances, respectively. There are no lumped sources driving the line; e.g., $V_G = 0$ in Fig. 7.3. (If there are lumped sources, the total response is just the superposition of the contributions from the lumped sources and from the field-induced sources.) $I(0)$ is the current in the left-hand load, and $I(s)$

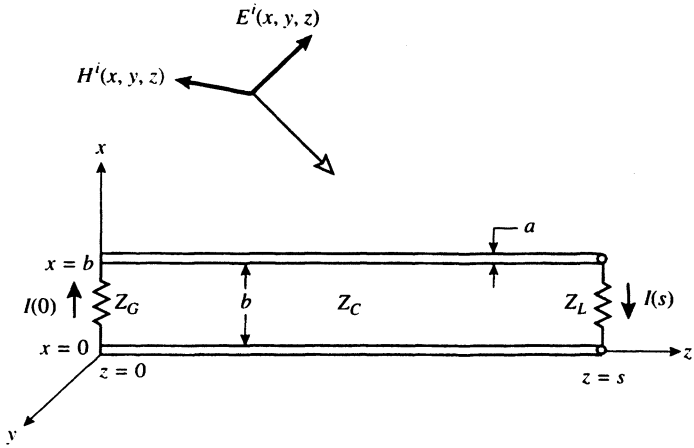

Figure 7.8 A nonuniform electromagnetic field incident on a two-wire transmission line.

is the current in the right-hand load. The load voltages are

$$V(0) = -Z_G I(0) \tag{7.65}$$

and

$$V(s) = Z_L I(s). \tag{7.66}$$

Figure 7.9 illustrates the components of the incident field that couple to, or excite, the transmission line. These incident field components induce distributed voltage sources along the conductors and along the terminations. The longitudinal (z-directed) electric field components incident on the two conductors, $E_z^i(b, z)$ and $E_z^i(0, z)$, excite both a *common-mode* and a *differential-mode* current on the line. See Section 7.2 and Fig. 7.2. The source of the common-mode current is the sum of the longitudinal E-fields on the two conductors, $E_z^i(b, z) + E_z^i(0, z)$. Common-mode or antenna-mode currents must be calculated using linear antenna theory. Tesche [13] calculated the common-mode and differential-mode current distributions on a 30-m long line. The common-mode current at the center of the line was larger than the differential-mode current by a factor of 20 (26 dB). The common-mode current distribution is zero at both ends of the line; common-mode currents do not flow in the load impedances.

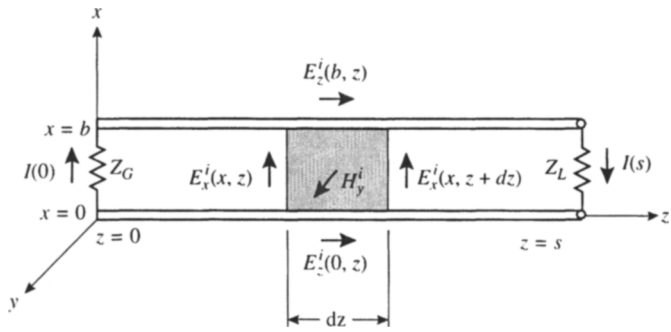

Figure 7.9 Components of the incident field that couple to the line.

The sources of differential-mode currents on the transmission line are the difference of the longitudinal E fields on the two conductors, $E_z^i(b, z) - E_z^i(0, z)$, and the transverse ($x$-directed) E-fields incident on the terminations, $E_x^i(x, 0)$ and $E_x^i(x, s)$. Only differential-mode currents flow in the loads and only differential-mode currents are predicted by transmission line theory.

Nonuniform-Field Excitation. The load currents on a lossless two-conductor line illuminated by a nonuniform electromagnetic field are [8], [9]

$$I(0) = \frac{1}{D}\int_0^s K(z)[Z_C \cos\beta(s-z) + jZ_L \sin\beta(s-z)]\,dz + \frac{1}{D}[Z_C \cos\beta s + jZ_L \sin\beta s]\int_0^b E_x^i(x,0)\,dx - \frac{Z_C}{D}\int_0^b E_x^i(x,s)\,dx \tag{7.67}$$

and

$$I(s) = \frac{1}{D}\int_0^s K(z)[Z_C \cos\beta z + jZ_G \sin\beta z]\,dz - \frac{1}{D}[Z_C \cos\beta s + jZ_G \sin\beta s]\int_0^b E_x^i(x,s)\,dx + \frac{Z_C}{D}\int_0^b E_x^i(x,0)\,dx \tag{7.68}$$

where the denominator D in (7.67) and (7.68) is

$$D = (Z_C Z_G + Z_C Z_L)\cos\beta s + j(Z_C^2 + Z_G Z_L)\sin\beta s \tag{7.69}$$

and where $K(z) = E_z^i(b,z) - E_z^i(0,z)$
$\beta = \omega/v = 2\pi/\lambda$ phase constant of line
v = phase velocity
$\omega = 2\pi f$
f = frequency, Hz.

Note: The load currents on a lossy line can be obtained from (7.67) to (7.69) by substituting $\cosh\gamma q$ for $\cos\beta q$ and $\sinh\gamma q$ for $j\sin\beta q$, where $q = z$ or s, as appropriate.

Plane-Wave Excitation. The expressions for the load currents excited by nonuniform fields in (7.67) and (7.68) reduce to much simpler forms when the illuminating field is a plane wave. Three cases of practical interest

serve to illustrate the theory: end-fire incidence, broadside incidence, and edge-fire incidence. These solutions are also derived by Paul [1] and in [9].

Case 1: End-Fire Incidence. In this case, the incident electric field E_x^i is parallel to the terminations and is traveling in the z direction. See Fig. 7.10. The incident magnetic field H_y^i is normal to the plane of the line. $E_z^i = 0$, and thus $K(z) = 0$. Also, since the electrical spacing of the conductors is small ($\beta b \ll 1$), E_x^i is uniform (constant) over the terminations and

$$\int_0^b E_x^i \, dx = bE_x^i \tag{7.70}$$

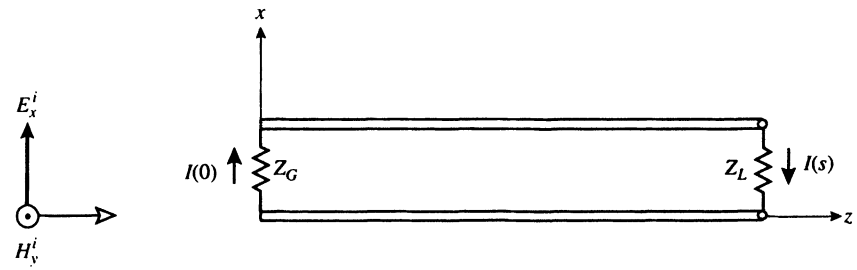

Figure 7.10 End-fire incidence.

With these simplifying conditions, the expressions for the load currents for end-fire incidence are

$$I(0) = j\frac{bE_x^i}{D}(Z_C + Z_L)\sin\beta s \tag{7.71}$$

and

$$I(s) = \frac{bE_x^i}{2D}(Z_C + Z_G)[(1 - \cos 2\beta s) + j\sin 2\beta s]. \tag{7.72}$$

Case 2: Broadside Incidence. In the case of broadside incidence shown in Fig. 7.11, the incident electric field E_x^i is parallel to the terminations and is traveling in the $-y$ direction. The incident magnetic field H_z^i is parallel to the plane of the line. That is, no magnetic flux lines link the plane of the transmission line when viewed as a rectangular loop. As in the case of end-fire incidence, $E_z^i = 0$ and thus $K(z) = 0$. And since E_x^i is uniform (constant) over the terminations, (7.70) holds.

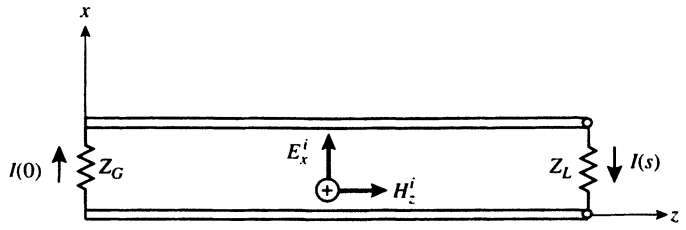

Figure 7.11 Broadside incidence.

The load currents for broadside incidence are

$$I(0) = -\frac{bE_x^i}{D}[Z_C(1 - \cos\beta s) - jZ_L \sin\beta s] \tag{7.73}$$

and

$$I(s) = \frac{bE_x^i}{D}[Z_C(1 - \cos\beta s) - jZ_G \sin\beta s]. \tag{7.74}$$

Note the symmetry in the expressions for the load currents.

Case 3: Edge-Fire Incidence. In this case, shown in Fig. 7.12, the incident electric field E_z^i is parallel to the conductors and is traveling in the $-x$ direction. The incident magnetic field H_y^i is normal to the plane of the line. Also, $E_x^i = 0$ and the terminations are not illuminated.

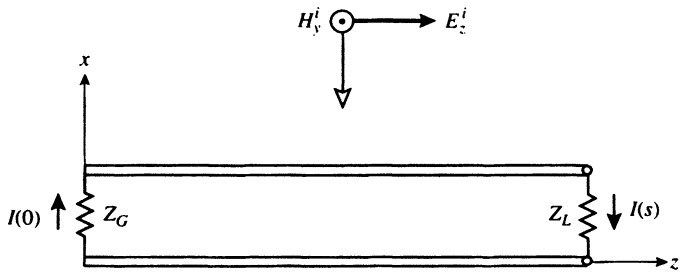

Figure 7.12 Edge-fire Incidence.

If the phase reference for the incident field is taken midway between the conductors at $x = b/2$, we have

$$E_z^i(b) = E_z^i \varepsilon^{+j\beta b/2}$$

and

$$E_z^i(0) = E_z^i \varepsilon^{-j\beta b/2}.$$

Then

$$K(z) = E_z^i \left[j2 \sin \frac{\beta b}{2} \right]. \tag{7.75}$$

The load currents for edge-fire incidence are given below. Again, note the symmetry in these expressions.

$$I(0) = -\frac{bE_z^i}{D} \left[\frac{\sin \frac{\beta b}{2}}{\frac{\beta b}{2}} \right] [Z_L(1 - \cos \beta s) - jZ_C \sin \beta s] \tag{7.76}$$

and

$$I(s) = -\frac{bE_z^i}{D} \left[\frac{\sin \frac{\beta b}{2}}{\frac{\beta b}{2}} \right] [Z_G(1 - \cos \beta s) - jZ_C \sin \beta s]. \tag{7.77}$$

Examples of load current spectrums on two-conductor lines of various lengths can be found in [1] and [9]. The results for an isolated two-conductor transmission line have limited application since this type of line is rarely used in practice. However, the two-conductor model is the basis for applications involving a conductor over a ground plane and related applications such as calculating the currents on the shield of coaxial and other shielded cables. These applications occur much more frequently in practice than applications involving two- conductor lines.

Conductor Over a Ground Plane

A single-conductor transmission line terminated at both ends to a perfectly conducting ground plane of infinite extent is illustrated in Fig. 7.13. The length of the line is s. The height of the conductor above the ground plane is h, and the diameter of the conductor is a. The terminating impedances are Z_G and Z_L.

The characteristic impedance of the line is

$$Z_C = \frac{60}{\sqrt{\varepsilon_r}} \ln \frac{4h}{a} \tag{7.78}$$

which is one-half the characteristic impedance of a two-conductor line with the conductors separated by $b = 2h$. ($2h$ is the spacing between the conductor and its image in the ground plane). See Table 7.1.

The total fields which illuminate the line are the sum of the incident (direct) fields and the ground-reflected fields. See Section 3.3, *Propagation*

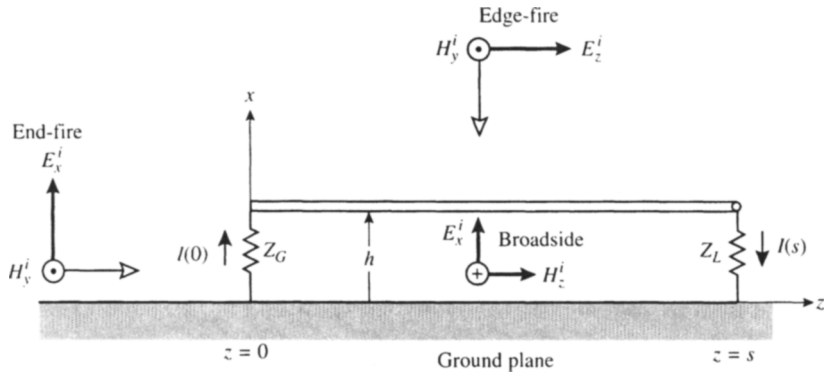

Figure 7.13 Single conductor over a ground plane.

over a Perfectly Conducting Plane. In the case of vertical polarization (end-fire and broadside incidence in Fig. 7.13), the wave reflection coefficient for a perfectly conducting plane is $\rho_v = +1$, and the total field is twice the incident field. That is,

$$E_x^{\text{total}} = 2E_x^i. \tag{7.79}$$

For horizontally polarized waves (edge-fire incidence in Fig. 7.13), the wave reflection coefficient at the perfectly conducting plane is $\rho_h = -1$. The total field on the conductor, taking the phase reference at the surface of the ground plane ($x = 0$), is

$$E_z^{\text{total}} = E_z^i \varepsilon^{+j\beta h} - E_z^i \varepsilon^{-j\beta h} \tag{7.80}$$

or

$$E_z^{\text{total}} = E_z^i [j2 \sin \beta h]. \tag{7.81}$$

Compare (7.81) with (7.75).

The solutions for the load currents for a single conductor above a ground plane can be obtained from the results for the two-conductor line by replacing b with $2h$. The solutions are given below for plane-wave excitation—specifically, for end-fire, broadside, and edge-fire incidence.

Common-mode or *antenna-mode* currents do not exist on a conductor over a ground plane. The *differential-mode* or *transmission-line-mode* current is the total current on the line.

Case 1: End-Fire Incidence. The expressions for the load currents for end-fire incidence are (see Fig. 7.13)

$$I(0) = j\frac{2hE_x^i}{D}(Z_C + Z_L) \sin \beta s \tag{7.82}$$

and

$$I(s) = \frac{hE_x^i}{D}(Z_C + Z_G)[(1 - \cos 2\beta s) + j \sin 2\beta s]. \tag{7.83}$$

As a practical matter, the incident and ground-reflected fields near a conducting ground plane cannot easily be separated. Only the total fields can be measured. E_x^{total} can be measured with a vertical monopole, and H_y^{total} can be measured with a loop antenna.

The load currents can be expressed in terms of the measured total electric field by making the following substitution in (7.82) and (7.83):

$$E_x^i = E_x^{\text{total}}/2. \tag{7.84}$$

The load currents can also be expressed in terms of the measured total magnetic field. Since the incident wave is plane wave, and assuming that the surrounding medium is air ($Zo = 120\pi$), we have

$$E_x^i = 120\pi H_y^i.$$

Also,

$$H_y^{\text{total}} = 2H_y^i.$$

We can then make the following substitution in (7.82) and (7.83):

$$E_x^i = 60\pi H_y^{\text{total}}. \tag{7.85}$$

Case 2: Broadside Incidence. Refer to Fig. 7.13. The load currents for broadside incidence, derived from the solutions for a two-conductor line, are

$$I(0) = -\frac{2hE_x^i}{D}[Z_C(1 - \cos \beta s) - jZ_L \sin \beta s] \tag{7.86}$$

and

$$I(s) = \frac{2hE_x^i}{D}[Z_C(1 - \cos \beta s) - jZ_G \sin \beta s]. \tag{7.87}$$

As in the case of end-fire incidence, the load currents may be expressed in terms of the measured total electric field by substituting (7.84) in (7.86) and (7.87).

The load currents may also be expressed in terms of the measured total magnetic field by making the following substitution equations in (7.86) and (7.87):

$$E_x^i = 60\pi H_z^{\text{total}}. \tag{7.88}$$

(This substitution is simply a way of expressing the incident electric field

in terms of the measured total magnetic field H_z^{total}, and does not imply that the magnetic flux links the plane of the line and contributes to the excitation of the line.)

Case 3: Edge-Fire Incidence. The load currents for edge-fire incidence are (see Fig. 7.13)

$$I(0) = -\frac{2hE_z^i}{D}\left[\frac{\sin\beta h}{\beta h}\right][Z_L(1-\cos\beta s) - jZ_C\sin\beta s] \tag{7.89}$$

and

$$I(s) = -\frac{2hE_z^i}{D}\left[\frac{\sin\beta h}{\beta h}\right][Z_G(1-\cos\beta s) - jZ_C\sin\beta s]. \tag{7.90}$$

As discussed previously, it is generally not possible to measure the *incident* field near a ground plane. In the case of a horizontally polarized field, it is also difficult to measure the *total electric field*, since this field is very small and has a strong dependence on position above the ground plane. (E_z is zero on the surface of the ground plane and increases rapidly with height above the plane.) On the other hand, the total magnetic field strength near the surface of the ground is twice the incident magnetic field strength and does not vary with height above the ground plane for heights small compared to a wavelength ($\beta h \ll 1$).

The load currents for edge-fire incidence may be expressed in terms of the measured total magnetic field by making the following substitution in (7.89) and (7.90):

$$E_z^i = 60\pi H_y^{\text{total}}. \tag{7.91}$$

Example 1: Short Conductor Over a Ground Plane. The load voltage spectrum of a physically short conductor over a ground plane normalized to the total magnetic field for edge-fire incidence is plotted in Fig. 7.14. This example might represent an interconnecting wire routed over a circuit board in an electronic enclosure, exposed to noise fields from external or internal sources. The dimensions of the line are

$s = 0.25$ m	line length
$h = 0.01$ m	height of conductor above ground
$a = 0.001$ m	diameter of conductor.

The characteristic impedance from (7.78) is 221.3 ohms, and the line is matched at both ends, i.e., $Z_G = Z_L = Z_C = 221.3$ ohms.

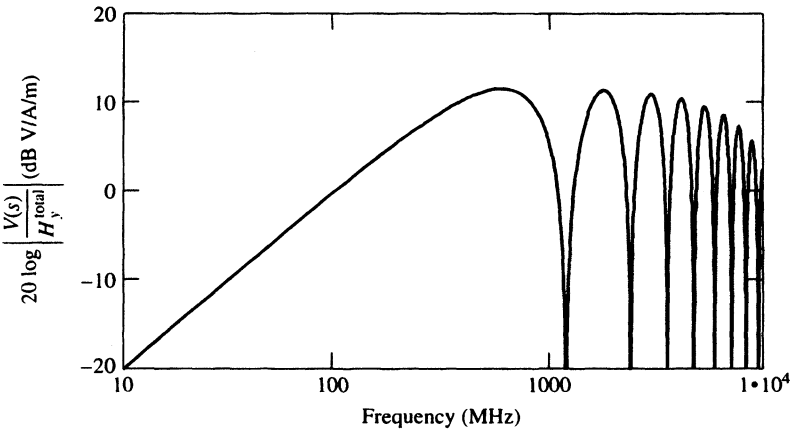

Figure 7.14 Load voltage spectrum for a short conductor over a ground plane in terms of the total magnetic field (horizontal polarization, edge-fire incidence).

The load voltage spectrum was calculated from (7.90) and (7.66), using (7.91) to express the response in terms of the total magnetic field. The resulting expression is

$$\frac{V(s)}{H_y^{\text{total}}} = -60\pi h \left[\frac{\sin \beta h}{\beta h}\right][(1 - \cos \beta s) - j \sin \beta s]. \tag{7.92}$$

The magnitude of (7.92) in dB is plotted in Fig. 7.14.

ELECTRICALLY SHORT LINE. When the transmission line is short compared to a wavelength ($\beta s \ll 1$), it can be approximated as a small rectangular loop antenna. The transmission line equations can be dispensed with and the load response can be calculated directly from Faraday's law. The open-circuit voltage of a loop is given by (2.3) in Chapter 2.

In the present example, the sending-end and receiving-end impedances are equal ($Z_L = Z_G$), and the voltage across each termination is one-half the open-circuit voltage.

From (2.3) in Chapter 2, the magnitude of the load voltage normalized to the total magnetic field is

$$\left|\frac{V(s)}{H_y^{\text{total}}}\right| = \frac{\omega \mu_o S}{2}. \tag{7.93}$$

In this example, the area of the line is

$$S = h \times s = 0.01 \times 0.25 = 0.0025 \text{ m}^2$$

and (7.93) reduces to

$$\left|\frac{V(s)}{H_y^{\text{total}}}\right| = 0.0098696 f_M \tag{7.94}$$

where f_M is the frequency in megahertz. This solution is much simpler than the transmission line formulation given by (7.92).

Equation (7.94) expressed in dB is

$$20 \log \left|\frac{V(s)}{H_y^{\text{total}}}\right| = -40.1 + 20 \log f_M. \tag{7.95}$$

The validity of the rectangular loop approximation for electrically short lines can be examined by comparing the numerical results of (7.95) with the load voltage spectrum in Fig. 7.14, which was calculated from the transmission line formulation in (7.92). This comparison shows that the rectangular loop approximation in (7.95) is accurate to within 0.6 dB when the electrical length of the line is one-quarter wavelength (240 MHz in this example). When the electrical length of the line is 0.1λ (120 MHz), the agreement is within 0.16 dB.

Example 2: Long Conductor Over a Ground Plane. The load current spectrum of a long conductor over a ground plane normalized to the total vertical electric field for end-fire incidence is plotted in Fig. 7.15. This example might represent an outdoor overhead wire or cable exposed to

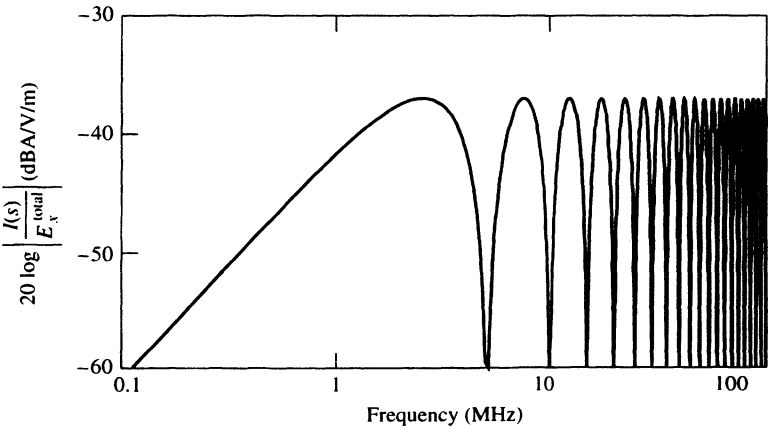

Figure 7.15 Load current spectrum for a long conductor over a ground plane in terms of the total vertical electric field (end-fire incidence).

ambient noise fields. The dimensions of the line are

$s = 30$ m	line length
$h = 3$ m	height of conductor above ground
$a = 0.01$ m	diameter of conductor.

The characteristic impedance from (7.78) is 425 ohms. The line is short circuited at the receiving end and matched at the sending end, i.e., $Z_L = 0$ and $Z_G = Z_C = 425$.

The spectrum in Fig. 7.15 was calculated from (7.83) using (7.84) to express the results in terms of the total vertical electric field.

7.9 RADIATION FROM TRANSMISSION LINES

Just as external electromagnetic fields can *induce* currents on transmission lines, the reciprocity principle dictates that currents on transmission lines will give rise to *radiated* electromagnetic fields. In general, both differential-mode and common-mode currents can exist on an isolated two-conductor or multiconductor line. In the case of a single conductor over a ground plane, the common-mode current is nonexistent; radiation is due solely to the differential-mode current. The currents on a conductor over a ground plane might represent leakage currents on the shield of a coaxial or other shielded cable.

Differential-mode or transmission line-mode currents do not radiate very efficiently. Since the differential-mode currents are equal in magnitude and oppositely directed (see Fig. 7.2), they tend to cancel; radiation is due to the space-phase difference between the conductors. Common-mode or antenna-mode currents on the conductors are equal in magnitude and flow in the same direction, resulting in much higher radiated field levels compared to differential-mode currents, as will be demonstrated below.

The radiated fields due to an arbitrary current distribution must be evaluated by integrating the current over the length of the line and the terminations. Besides the challenge of trying to accurately determine or specify the magnitude and phase of the current distribution, the resulting mathematics can be quite complex. However, if the transmission line is electrically short (approximately one-quarter wavelength or shorter), it can be modeled as a small loop antenna for differential-mode radiation, and as a pair of short dipoles for common- mode radiation. The analysis in this section assumes that the lines are electrically short.

Two-Conductor Line

Differential-Mode Radiation. The radiated fields due to differential-mode currents on an electrically short two-conductor transmission line, modeled as a small rectangular loop antenna, are illustrated in Fig. 7.16. As previously, the length of the line is s and the spacing between the conductors is b. The area of the transmission line (rectangular loop) is

$$S = bs \qquad \text{m}^2. \tag{7.96}$$

I_{DM} is the normal signal current on the line due to sources at either end of the line and can be predicted from straightforward transmission line theory. See Section 7.7. The differential-mode current can also be measured with a current probe. This measurement may be conveniently performed at either termination where the common-mode current is zero. That is, since the line is assumed to be electrically short ($s/\lambda \ll 1$), the differential-mode current is uniform in amplitude and phase (constant) everywhere on the line.

In Fig. 7.16, r is the distance from the transmission line to the field point. It is assumed that r is much greater than the length of the line ($r \gg s$). The radiated fields are obtained directly from the solutions for

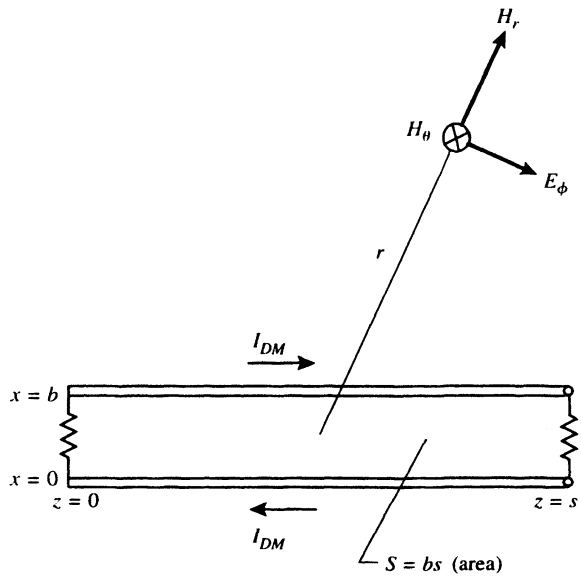

Figure 7.16 Radiated fields from differential-mode currents on a two-conductor line.

a small loop given in Section 2.10. The coordinate system is the same as in Fig. 2.15. We restrict the solutions to the fields in the same plane as the transmission line, i.e., $\theta = 90°$ in Fig. 2.15.

FAR FIELDS. The far-field transverse electric field component, from (2.72) is

$$E_\phi = \frac{30 I_{DM} S\beta^2}{r} \varepsilon^{-j\beta r} \quad \text{V/m} \tag{7.97}$$

or

$$\boxed{E_\phi = 1.316 \times 10^{-2} \frac{I_{DM} S f_M^2}{r} \varepsilon^{-j\beta r} \quad \text{V/m}} \tag{7.98}$$

where f_M is the frequency in MHz and S is the area of the line. This is the same result obtained by Paul and Bush [14] and Paul [15], who modeled the conductors as infinitesimal dipoles.

The far-field transverse magnetic field component, from (2.73) is

$$H_\theta = \frac{I_{DM} S\beta^2}{4\pi r} \varepsilon^{-j\beta r} \quad \text{A/m} \tag{7.99}$$

or

$$\boxed{H_\theta = 3.5 \times 10^{-5} \frac{I_{DM} S f_M^2}{r} \varepsilon^{-j\beta r} \quad \text{A/m.}} \tag{7.100}$$

REACTIVE NEAR FIELDS. The reactive near-field components due to the differential-mode current, from (2.72) to (2.74), are

$$\boxed{E_\phi = -j0.628 \frac{I_{DM} S f_M}{r^2} \varepsilon^{-j\beta r} \quad \text{V/m}} \tag{7.101}$$

$$\boxed{H_\theta = \frac{I_{DM} S}{4\pi r^3} \varepsilon^{-j\beta r} \quad \text{A/m}} \tag{7.102}$$

and

$$\boxed{H_r = \frac{I_{DM} S}{2\pi r^3} \varepsilon^{-j\beta r} \quad \text{A/m.}} \tag{7.103}$$

Common-Mode Radiation. The radiated fields due to common-mode currents on an electrically short two-conductor transmission line are illustrated in Fig. 7.17. The conductors are modeled as two short dipole antennas spaced a distance b apart. As previously, the length of the line (short dipoles) is s. A triangular current distribution is assumed on the

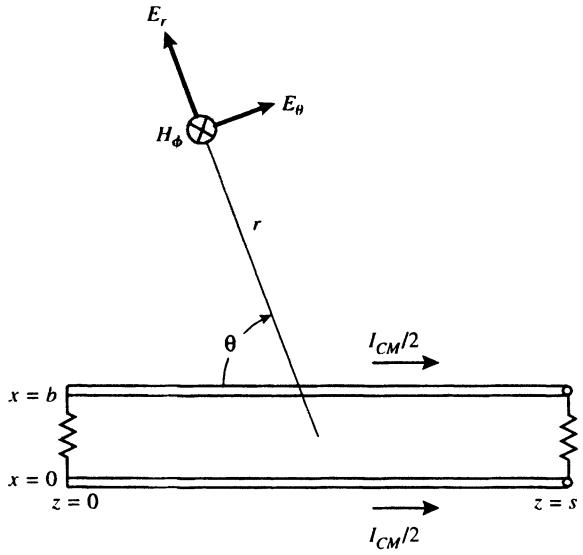

Figure 7.17 Radiated fields from common-mode currents on a two-conductor transmission.

short dipoles, which is representative of common-mode currents in that the current is zero at the ends of the line. The current at the midpoint of each conductor is $I_{CM}/2$. A current probe clamped around both conductors at the midpoint of the line would read I_{CM}.

In Fig. 7.17, r is the distance from the transmission line to the field point. It is assumed that r is much greater than the length of the line ($r \gg s$). The radiated fields are obtained from the solutions for a short dipole given by (2.68) to (2.70), Section 2.9. (These equations must be divided by 2 since a triangular current distribution is assumed in the present application.) The coordinate system is the same as in Fig. 2.12. Again, we restrict the solutions to the fields in the same plane as the line.

FAR FIELDS. The far-field transverse electric field component, from (2.68), is

$$\boxed{E_\theta = j0.3125\frac{I_{CM}sf_M \sin\theta}{r}\varepsilon^{-j\beta r} \quad \text{V/m}} \tag{7.104}$$

where f_M is the frequency in MHz and s is the length of the line. This result is lower than that obtained by Paul and Bush [14] and Paul [15] by a factor of 2. These investigators modeled the conductors as infinitesimal dipoles with a uniform current distribution.

The far-field transverse magnetic field component, from (2.70) is

$$H_\phi = j8.35 \times 10^{-4} \frac{I_{CM} s f_M \sin\theta}{r} \varepsilon^{-j\beta r} \quad \text{A/m.} \tag{7.105}$$

REACTIVE NEAR FIELDS. The reactive near-field components due to the common-mode current, from (2.68) to (2.70), are

$$E_\theta = -j716 \frac{I_{CM} s \sin\theta}{f_M r^3} \varepsilon^{-j\beta r} \quad \text{V/m} \tag{7.106}$$

$$E_r = -j1432 \frac{I_{CM} s \cos\theta}{f_M r^3} \varepsilon^{-j\beta r} \quad \text{V/m} \tag{7.107}$$

and

$$H_\phi = 0.0398 \frac{I_{CM} s \sin\theta}{r^2} \varepsilon^{-j\beta r} \quad \text{A/m.} \tag{7.108}$$

COMPARISON OF DM AND CM RADIATION. In order to compare the relative magnitudes of the radiated fields due to differential-mode and common-mode currents, consider a two-conductor line with the following dimensions (see Figs. 7.16 and 7.17):

$s = 0.25$ m	line length
$b = 0.01$ m	conductor spacing
$S = b \times s = 2.5 \times 10^{-3}$ m^2	area.

The far-field transverse E field due to differential-mode currents, from (7.98), is

$$|E_{DM}| = \frac{3.29 \times 10^{-5} I_{DM} f_M^2}{r}. \tag{7.109}$$

The far-field transverse E field due to common-mode currents, from (7.104) with $\theta = 90°$, is

$$|E_{CM}| = \frac{7.8 \times 10^{-2} I_{CM} f_M}{r}. \tag{7.110}$$

The ratio of the fields radiated by common-mode and differential-mode currents is

$$\frac{|E_{CM}|}{|E_{DM}|} = \frac{2.37 \times 10^3}{f_M} \frac{I_{CM}}{I_{DM}}. \tag{7.111}$$

If the common-mode and differential-mode currents are equal, at a frequency of 100 MHz, for example,

$$\frac{|E_{CM}|}{|E_{DM}|} = 23.7 \quad \text{or} \quad 27.5 \text{ dB}. \tag{7.112}$$

That is, the radiated E field due to the common-mode current is 27.5 dB greater than the radiated E field due to the differential-mode current. This result is consistent with the measurements reported by Paul and Bush [14], [15]. While it is unlikely that the common-mode and differential-mode currents would be equal in a practical application, this analysis at least shows that common-mode currents will, most likely, be the predominant source of radiation.

Conductor over A Ground Plane

A single-conductor transmission line terminated at both ends to a perfectly conducting ground plane is shown in Fig. 7.18. The length of the line is s and the height of the conductor above the ground plane is h. The current on the conductor is I_{DM}. The current distribution is uniform since the line is assumed to be electrically short.

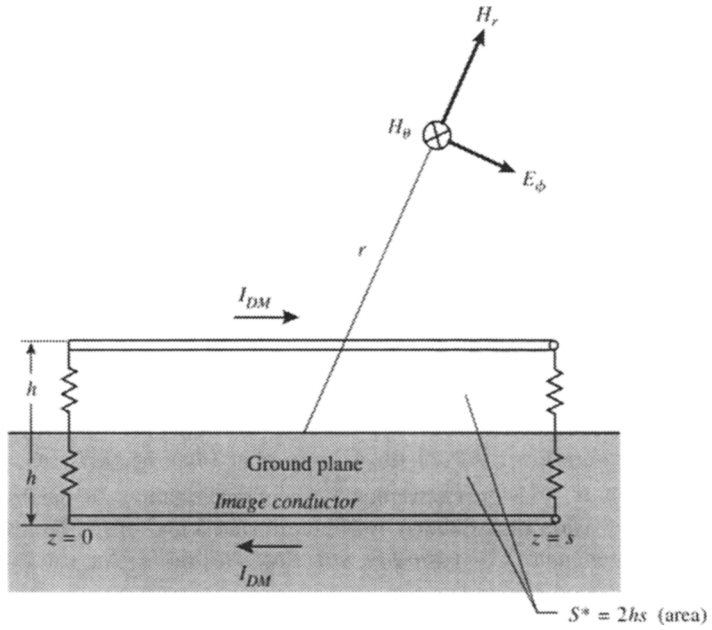

Figure 7.18 Radiated fields from a single conductor over a perfectly conducting ground plane (image formulation).

The conductor and its image in the ground plane are spaced a distance $2h$ apart and form a rectangular loop antenna. This problem is identical to the one shown in Fig. 7.16 for the radiated fields from differential-mode currents on a two-conductor line if the conductor spacing b in Fig. 7.16 is replaced by $2h$.

Then the radiated fields from a conductor over a ground plane are given by (7.97) to (7.103) by replacing

$$S = bs \qquad \text{m}^2 \tag{7.96}$$

with

$$\boxed{S^* = 2hs \qquad \text{m}^2.} \tag{7.113}$$

REFERENCES

[1] C. R. Paul, *Analysis of Multiconductor Transmission Lines*, A Wiley-Interscience Publication, John Wiley & Sons, New York, 1994.

[2] B. C. Wadell, *Transmission Line Design Handbook*, Artech House, Inc., Norwood, Massachusetts, 1991.

[3] W. C. Johnson, *Transmission Lines and Networks*, McGraw-Hill Book Company, New York, 1950.

[4] R. E. Collin, *Field Theory of Guided Waves*, IEEE/OUP Series on Electromagnetic Wave Theory, IEEE Press Selected Reprint Volume, IEEE Press, Piscataway, NJ.

[5] T. Itoh, *Transmission Lines*, Chapter 29 in *Reference Data for Engineers: Radio, Electronics, Computer, and Communications*, Howard W. Sams & Company, Division of Macmillan, Inc., Indianapolis, Indiana, seventh edition, fifth printing, 1989.

[6] R. A. Chipman, *Theory and Problems of Transmission Lines*, Schaum's Outline Series, McGraw-Hill Book Company, New York, 1968.

[7] C. D. Taylor, R. S. Satterwhite, and C. W. Harrison, Jr., "The Response of a Terminated Two-Wire Transmission Line Excited by a Nonuniform Electromagnetic Field," *IEEE Transactions on Antennas and Propagation* (communication), vol. AP-13, no. 6, November 1965, pp. 987–989.

[8] A. A. Smith, Jr., "A More Convenient Form of the Equations for the Response of a Transmission Line Excited by Nonuniform Fields," *IEEE Transactions on Electromagnetic Compatibility*, vol. EMC-15, no. 3, August 1973, pp. 151–152.

[9] A. A. Smith, Jr., *Coupling of External Electromagnetic Fields to Transmission Lines*, first ed., John Wiley & Sons, New York, 1977, second ed., Interference Control Technologies, Gainesville, VA, 1987.

[10] C. R. Paul, "Frequency Response of Multiconductor Transmission Lines Illuminated by an Incident Electromagnetic Field," *IEEE Transactions on Electromagnetic Compatibility*, vol. EMC-18, no. 4, November 1976, pp. 183–190.

[11] A. K. Agrawal, H. J. Price, and S. H. Gurbaxani, "Transient Response of Multiconductor Transmission Lines Excited by a Nonuniform Electromagnetic Field," *IEEE Transactions on Electromagnetic Compatibility*, vol. EMC-22, no. 2, May 1980, pp. 119–129.

[12] F. Rachidi, "Formulation of the Field-to-Transmission Line Coupling Equations in Terms of Magnetic Excitation Field," *IEEE Transactions on Electromagnetic Compatibility*, vol. EMC-35, no. 3, August 1993, pp. 404–407.

[13] F. M. Tesche, M. V. Ianoz, and T. Karlsson, *EMC Analysis Methods and Computational Models*, A Wiley-Interscience Publication, John Wiley & Sons, New York, 1997.

[14] C. R. Paul and D. R. Bush, "Radiated Emissions From Common-Mode Currents," *IEEE Symposium on Electromagnetic Compatibility*, Atlanta, GA, August 1987.

[15] C. R. Paul, "A Comparison of the Contributions of Common-Mode and Differential-Mode Currents in Radiated Emissions," *IEEE Transactions on Electromagnetic Compatibility*, vol. EMC-31, no. 2, May 1989, pp. 189–193.